

ORIGINAL RESEARCH OPEN ACCESS

Predicting the Fault-Ride-Through Probability of Inverter-Dominated Power Grids Using Machine Learning

 Christian Nauck¹  | Anna Büttner¹ | Sebastian Liemann² | Frank Hellmann¹ | Michael Lindner¹
¹Potsdam Institute for Climate Impact Research, Potsdam, Brandenburg, Germany | ²Institute of Energy Systems, Energy Efficiency and Energy Economics (ie3), Technical University of Dortmund, Dortmund, Germany

Correspondence: Frank Hellmann (hellmann@pik-potsdam.de)

Received: 11 November 2025 | **Revised:** 20 January 2026 | **Accepted:** 7 February 2026

ABSTRACT

Assessing and mitigating risks in future power grids requires comprehensive analysis of their dynamic behaviour. Probabilistic stability analyses, which evaluate large ensembles of disturbances, are well-suited for this purpose and became mandatory for many grid operators. However, the computational costs of simulations impose strict limits on the number of configurations that can be evaluated. This study demonstrates how machine learning (ML) can address this challenge by enabling efficient prioritization of scenarios for detailed analysis in probabilistic dynamic stability assessments. We apply fault-ride-through probability—a practical metric measuring the likelihood of all grid components remaining within operational bounds after a fault—to show how ML can bridge the gap to real-world applications. A new dataset comprising thousands of dynamic simulations of synthetic power grids is generated to train ML models. Results reveal that ML models not only accurately predict fault-ride-through probabilities but also effectively rank the criticality of buses, identifying components most likely to destabilize the system and requiring further analysis. Importantly, the models generalize well to the IEEE-96 Test System, underscoring their robustness and scalability. This work highlights the transformative potential of ML in enabling efficient, scalable probabilistic stability studies, paving the way for integration into contingency screening for real-world grid operations.

1 | Introduction

The transition towards renewable energy sources (RESs) introduces significant challenges to power grid stability, particularly in future grids that aim for nearly 100% RES integration. These power grids face reduced inertia [1], decentralized [2], volatile [3] production and decreased short-circuit levels [4]. As a result, understanding and analysing the dynamic behaviour of such systems is crucial. Since RESs are predominantly integrated through power electronic inverters, the role of grid-forming inverters, which stabilize power grids without relying on conventional generation, has become increasingly important [5].

Ensuring stable grid operation, especially under these conditions, requires comprehensive dynamic stability assessments, typically

performed via computationally intensive non-linear simulations. Non-linear stability analyses are particularly pertinent due to the inherent non-linear nature of power grids [6]. Probabilistic stability analyses, which evaluate large ensembles of disturbances using Monte Carlo simulations, have recently been mandated by the European Network of Transmission System Operators for Electricity (ENTSO-E) [7, 8]. However, the computational burden of these simulations is substantial. The vast number of possible configurations and scenarios makes exhaustive simulation-based analysis impractical, increasing the risk of overlooking critical scenarios.

To address the challenges of resource-intensive simulations, machine learning (ML) offers a promising approach. A comprehensive literature review demonstrates that ML has achieved

This is an open access article under the terms of the [Creative Commons Attribution](https://creativecommons.org/licenses/by/4.0/) License, which permits use, distribution and reproduction in any medium, provided the original work is properly cited.

© 2026 The Author(s). *IET Generation, Transmission & Distribution* published by John Wiley & Sons Ltd on behalf of The Institution of Engineering and Technology.

significant success across a range of power system applications [9, 10]. While recent studies have applied ML to assess the reliability of medium-voltage grids [11], these methods often overlook system dynamics. Probabilistic static assessments are well established [12] and remain an active area of research, with ML techniques increasingly used to predict probabilistic stability, for example, voltage stability [13]. In dynamic contexts, ML has been employed to forecast individual transients [14–16], aiming to reduce reliance on costly simulations. Additionally, there is growing interest in analysing the dynamic stability of inverter-dominated power grids [17, 18] and in leveraging ML for dynamic behaviour prediction [19].

Despite these advances, the literature review reveals that no existing study has applied ML to predict probabilistic dynamic stability in realistic, inverter-dominated power grids using operationally relevant metrics. This work addresses this gap by directly predicting the outcomes of full probabilistic stability assessments, thereby contributing to the critical challenge of enabling probabilistic stability evaluations required by grid operators.

Recent studies have demonstrated the feasibility of predicting probabilistic dynamic stability measures in physical oscillator networks [20, 21]. While these works provide valuable insights, they should only be used as inspiration because they fall short of addressing the complexities of real-world power grids. They lack accurate representations of realistic power grid dynamics, for example, neglecting voltage dynamics, and fail to incorporate stability metrics directly relevant to practical applications, such as those mandated by grid operators. Moreover, these models do not explicitly account for inverter-based generation, which is a defining feature of RES-dominated systems and plays a pivotal role in their dynamic behaviour. By addressing these gaps, our study directly tackles the challenges of modern power grids, making it highly relevant for advancing probabilistic stability analyses in real-world applications.

Building on the methodological foundations of [20, 21], this study pioneers the application of ML to predict fault-ride-through capabilities, an essential dynamic stability metric, relevant for assessing the dynamic stability in inverter-dominated power grids. To measure the fault-ride-through capabilities, the concept of survivability [22] is applied, which uses Monte Carlo simulations to estimate the probability that a system remains within operational limits following a disturbance. This approach has been effectively used in previous studies [23, 24], such as assessing fault-ride-through probabilities in active distribution grids [25].

The proposed ML framework aims to identify scenarios and components most likely to cause dynamic stability issues, thereby supporting targeted analyses and serving as a contingency screening tool for grid operators. To the best of the authors' knowledge, this is the first study to leverage ML techniques for predicting probabilistic dynamic stability in realistic grid environments using metrics directly aligned with operational decision-making. By addressing practical challenges, this work marks a significant step toward translating conceptual research into actionable solutions for modern power systems.

Graph neural networks (GNNs) are widely used for power grid assessments due to their ability to model relational and

topological information [26–29]. In this study, Dirac–Bianconi graph neural networks (DBGNNs) [30] are employed as a novel GNN layer capable of capturing complex topological structures—including long-range dependencies—while incorporating both node and edge features, which are key aspects for this analysis. To provide a clearly justified comparison and highlight the importance of topological information, a simpler baseline is also evaluated: gradient-boosted trees (GBT), which are known to perform well on tabular data and, in this context, use only local bus features. Results demonstrate that incorporating graph data into ML models significantly improves prediction accuracy compared to models relying solely on local bus data. Furthermore, ML models trained on synthetic grids generalize well to other grid topologies, such as the IEEE-96 test grid, which was excluded from the training dataset.

The following sections provide concise summaries of the key concepts and methodologies, including background on probabilistic stability assessments (Section 2.1) and machine learning approaches (Section 2.2). The main contributions of this study are:

1. The creation and open release of a large, realistic dataset of synthetic power grids, including detailed dynamic simulation results for fault-ride-through behaviour in inverter-dominated grids (Section 3 and Section 5.1).
2. The first demonstration that graph-based ML models can accurately predict non-linear, operationally relevant stability measures in inverter-dominated power grids, outperforming strong tabular-data baselines (Section 5.2). This establishes these methods as strong candidates for accurate contingency screening.
3. The first demonstration that graph-based ML models can accurately predict non-linear, operationally relevant stability measures in inverter-dominated power grids, outperforming strong tabular-data baselines (Section 5.2). The ML models effectively rank critical components and prioritize scenarios for detailed analysis, establishing ML as a powerful tool for efficient contingency screening in large-scale grid operations.

The results of this study demonstrate the potential of our approach as a tool for detecting vulnerabilities and screening potentially critical contingencies within power grids. By providing a ranked output of components most susceptible to failure, it supports grid operators, particularly those managing limited resources, in identifying which configurations require targeted and detailed analysis.

2 | Theoretical Background

2.1 | Probabilistic Stability Analysis

Analysing power grids under extreme conditions helps to understand the system dynamics and to identify critical components that may fail. Typically, a binary classifier is used, meaning that a scenario can either be stable or unstable according to operational bounds or grid codes. While studying extreme scenarios is important, exclusively focusing on a few such scenarios can be limiting [31]. When studying a small set of scenarios, the system

stability could be overestimated, and detrimental situations could be overlooked. To avoid this problem, one can study randomly generated scenarios in a Monte Carlo simulation.

Such studies are so-called probabilistic stability analyses. They are established for static power flow studies [12] and have recently been mandated by the European Network of Transmission System Operators for Electricity (ENTSO-E) [8]. In probabilistic stability analyses, a large set of faults is randomly selected to analyse the response of a system. Probabilities of failures, instead of binary classifiers, can then be associated with different grid configurations.

Probabilistic approaches are also of increasing interest when analysing the dynamics [8]. They are especially vital in dynamic contexts as power systems are complex, non-linear systems [6]. Identifying the most critical scenarios for non-linear systems is challenging, as a fault with a lower magnitude could lead to a more detrimental system response. A detailed analysis of the non-linear dynamics of the studied dataset shows this effect (Section 5.1). These results clearly underline the need for probabilistic approaches.

The combination of probabilistic analysis with dynamic simulations requires especially expensive computations, which limited their applications in the past. The advancing capabilities of ML-based approaches expand their applicability by enabling a rapid pre-analysis of numerous scenarios. These methods allow for ranking scenarios based on their susceptibility to failure, identifying those requiring more detailed analysis. This work focuses on the fault-ride-through probability p_{frit} , which has previously been studied in [25] and will be introduced in the following sections.

2.1.1 | Fault-Ride-Through Probability

Here, fault-ride-through capabilities refer to the ability of all power grid components to stay within a ride-through curve after a fault at a bus has been cleared. They are considered an essential measure of stability, especially for inverters. Examples are research projects focusing on the operation of power grids under 100% inverters [32], guidelines for grid forming behaviour [33] or installation rules for power generating facilities [34]. Fault-ride-through curves are essential to maintain system and equipment within operational bounds, preventing grid instability and hardware damage. Example trajectories with ride-through curves are illustrated in Figure 3, with details on the ride-through curves in Section 3.2.

Instead of studying a small set of faults, fault-ride-through statistics are analysed. In the following, we will refer to the grid state after the occurrence and clearance of a fault as post-clearance states. The fault-ride-through probability p_{frit} is defined by:

$$p_{\text{frit}} = \frac{V^*}{V_t}, \quad (1)$$

where V^* is the number of randomly generated post-clearance states for which the transients stay within a ride-through curve,

and V_t is the total number of investigated states. Hence, a system that never exceeds a ride-through curve has $p_{\text{frit}} = 1$.

The fault-ride-through probability is a particular case of the so-called survivability [22], that has been applied to power grids successfully in the past [23–25].

In this work, we consider post-clearance states for individual buses, resulting in a fault-ride-through probability for each bus. This allows us to predict critical components with a high probability of failing after fault clearing.

2.2 | Machine Learning

Machine learning (ML) has been widely applied to various power grid challenges, as reviewed in multiple studies [9, 10, 35].

The choice of ML methods depends on the specific application. Conventional approaches, such as gradient-boosted trees and deep neural networks, are effective in systems with fixed topologies. In contrast, GNNs are particularly well-suited where topological properties are essential or when topologies change frequently. While conventional ML methods focus solely on nodal (or bus) features, GNNs can incorporate the entire graph structure. In this work, methods based solely on nodal features will be referred to as non-graph ML.

GNNs are recognized as the preferred solution for problems that rely on topological properties, as they consider the entire graph structure as input. By incorporating the graph via the adjacency matrix A or similar representations, GNNs can aggregate information from the spatial neighbourhood. This capability makes GNNs particularly useful for power grid-related tasks where the topology significantly impacts outcomes, such as in cases of network congestion. Conventional ML methods that do not account for the topological structure often underperform in such scenarios. One of the major breakthroughs in GNNs was the development of the graph convolutional layer (GCN), which is defined as [36]:

$$H = \sigma(\overline{AX}\Theta), \quad (2)$$

where H represents the output, σ is the activation function σ , using the input features, Θ are the learnable parameters, and \overline{A} is the normalized and modified version of the adjacency matrix A . Multiple GCN layers can be applied consecutively to consider information beyond immediate neighbours, capturing the larger surroundings of the buses.

The Dirac–Bianconi GNN (DBGNN) layer, introduced in [30], is a more advanced GNN that simultaneously considers node and edge features, both of which are present in our dataset. DBGNN is particularly effective at tasks where long-range interactions are crucial. For power grids, the importance of such long-range dependencies was highlighted by [37], making DBGNN an excellent choice for our analysis. Furthermore, its strength for prediction tasks on simplified synthetic power grid models have already been demonstrated in [30]. DBGNNs are discussed in detail in Section A.4.

TABLE 1 | The used parameterizations for the grid-forming inverters.

Name	Time constants	τ_p [s]	Source
NF1	Low	0.5	Schiffer et al. [39]
NF2	Medium	1.0	Kogler et al. [40]
NF3	High	5.0	Büttner et al. [42]

3 | Dataset Generation

Generally, ML methods require sufficiently large datasets to achieve accurate predictions. Probabilistic stability analyses, based on dynamic simulations, of real-sized power grids with thousands of buses will remain unfeasible in the near future. The computational cost of these assessments scales at least quadratically with the number of buses. The quadratic factor is caused by more expensive computations per fault scenario and the increasing number of faults that must be analysed.

This complicates the generation of a sufficiently large dataset for machine learning applications. To tackle this issue, instead of using single real-sized power grids, we rely on numerous smaller synthetic ones. Furthermore, by considering numerous smaller grids, the various topological structures existing in real-sized power grids are included in the dataset.

The following sections describe the dataset generation process, including the generation of the ensemble of synthetic power grids and the dynamic simulations.

3.1 | Synthetic Power Grids

The synthetic power grid framework introduced in [38], depicted in Figure 1, was used to generate the dataset. The framework generates power grids based on input parameters such as grid size and models for power lines and buses. It ensures that all validation criteria are met before returning a synthetic grid ready for dynamic simulation.

For the dataset, power grids of different sizes are generated. The number of buses varies between 70 and 80, which is sufficiently large to include topological effects but still computationally feasible.

The energy sources in the power grids comprise 100% RESs, with 50% of the generators connected via grid-forming inverters and the remaining 50% via grid-following inverters. All grid-forming inverters are droop-controlled inverters [39] and are modelled using the so-called normal-form model [40], which has been validated by measurements performed in a power-hardware-in-the-loop laboratory [41]. Grid-following inverters and loads are modelled as PQ-buses.

Three parameter sets for grid-forming inverters, drawn from the literature [39, 40, 42], are summarized in Table 1. These parameter sets vary only in the time constants τ_p of the active

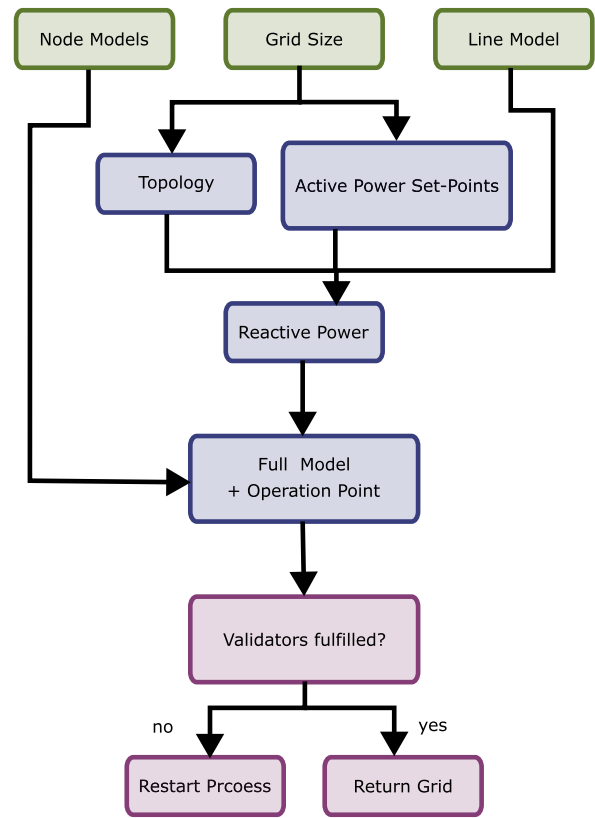


FIGURE 1 | The structure of the power system generation algorithm shows the generation based on the chosen input parameters. Before the algorithm returns the power grid, its behaviour is validated to fulfil the stability criteria of real power grids.

power low-pass filter in the droop control. Buses with larger time constants are anticipated to have a greater fault-ride-through probability, as their faster response increases the likelihood of remaining within the ride-through curve during the critical first milliseconds following fault clearance.

Grid-following inverters and loads are modelled as PQ-buses, while the Pi-model is used to model the transmission lines.

The algorithm introduced in [43] generates the power grid topologies. The line- and shunt admittances are calculated according to the standard line parameters for transmission systems with a voltage of 380 kV published by the German energy agency [44].

For a realistic distribution of active power demand and supply, the *ELMOD-DE* dataset [45], a dispatch model for the German EHV transmission system, is used. Following [46], which builds on [45], a bimodal distribution for the net power at a bus is employed. The reactive power is distributed using a voltage stability objective [47]. The reactive powers at the buses are adjusted to fulfil the desired voltage magnitudes by solving a load flow problem.

Before a power grid is analysed further, a small signal stability analysis is performed to guarantee that the grids are linearly stable and it is validated that no lines in the grid are overloaded during normal operation.

3.2 | Ride-Through Curves

This work will consider ride-through curves for the bus voltages and frequencies. To enable direct comparisons with prior work in [25], we use a variant of the medium and high voltage fault-ride through curves of the German technical connection rules for inverter based generation. Overvoltage curves follow [34] and undervoltage curves follow [48]. The frequency ride-through curve is given by constant symmetric thresholds for the frequency of $[-2, +2]$ Hz. While we consider post-clearance states for individual buses, the fault-ride-through curves are always considered for all buses. This means that the fault-ride-through probability is a measure that explicitly considers the dynamics of the entire grid. The ride-through curves are illustrated in Figure 3.

3.3 | Simulation Setup

When generating the dataset and computing the fault-ride-through probability, there is a compromise between low statistical and numerical errors and the computational costs. 1000 grids with 70 to 80 buses are generated. For each network 1000 post-clearance states per bus are analysed.

Explicitly modelling every fault to generate these states requires a significant additional modelling effort and computational resources. Instead, so-called Sobol sequences, which are enhanced quasi Monte-Carlo samples [49] and the ambient forcing algorithm [42] have been employed.

As a first step, the Sobol sequences, which are quasi-random and well-distributed points sequences, are used to sample the space of post-clearance states. The magnitude of the voltage at one of the buses is sampled in a regime of $[0,1]$ p.u.. Furthermore, the phase angle of the bus is drawn from the regime of $[0, +2\pi]$. An additional frequency fault in an interval of $[-1, +1]$ Hz is applied for grid-forming components. In the second step, the ambient forcing algorithm [42] is employed as an initialization technique to ensure all algebraic constraints are fulfilled.

Higher-order implicit differential algebraic equations solvers are used with low error tolerances to achieve low standard errors of ± 0.02 for the probabilistic measures. The total computation cost for generating the dataset is roughly 50,000 CPU hours. Details on the software used to generate the dataset can be found in Appendix A.2. The results of the numerical study can be found in Section 5.1.

3.4 | IEEE 96-RTS Test System

The IEEE 96-RTS test case [50] was chosen as a test system to validate if the ML models can generalize to a different power grid model. The IEEE test system is not used for training and features a fundamentally different topology, with its own active power set-points and load distribution. Hence, the performance is evaluated on a configuration entirely new to the ML models which is a challenge for accurately predicting its stability.

The IEEE test case has been updated to include converter interfaced generation, which is not present in the original system.

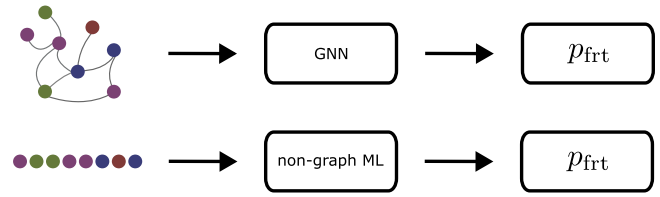


FIGURE 2 | Training setup: The GNN gets the full power grid as input (bus features, line features, and the topology), whereas the nodal features are the only input for the non-graph ML methods. In all cases, the outputs are the nodal fault-ride-through probability (p_{frt}).

All buses that generate power are assumed to be grid-forming inverters and are therefore modelled by the normal-form. The parameterization from Table 1 is used as well. Loads are modelled as PQ-buses.

The line parameters of the system are updated to match the synthetic grids introduced in Section 3.1. The geographical locations of buses and lines given in the original IEEE test case are kept.

Finally, the probabilistic non-linear stability of the test system is calculated using the same procedure as for the synthetic grids.

4 | Machine Learning Setup

4.1 | Training Setup

To evaluate the capabilities of ML to predict p_{frt} via nodal regression, we compare GNNs with non-graph ML predictions using linear regression (linreg) and GBT. By non-graph ML, we mean ML methods that do not consider the topology but purely rely on nodal features. The two general approaches are visualized in Figure 2. The mean squared error is used and evaluated as a loss function on all buses except for the slack bus, which in our model is always stable. The following subsection describes the preprocessing of the dynamical results for the ML predictions.

4.2 | Feature Preparation

The node type (normal-form, load, slack) is represented using one-hot encoding, resulting in three binary input variables. All bus types have standard active and reactive power (P, Q) as nodal features, and the grid-forming inverters have one additional input parameter: the time constant τ_p . To have the same number of input parameters for all bus types, 0 is used for τ_p for load and slack buses.

To improve the predictive power of all ML methods, we compute three additional nodal features based on the surrounding line properties of each bus k . The three line parameters are the conductance G_{km} , susceptance B_{km} and the shunt susceptance $B_{k,\text{sh}}$. Computing the sums yields: $G_k = \sum_m G_{km}$, $B_k = \sum_m B_{km}$ and $B_{k,\text{sh}} = \sum_m B_{k,\text{sh}}$.

This leads to nine input features in total that are directly used for GBT and linear regression as the only input and, in the case of the GNNs, as nodal features.

Further, the input features may be scaled as a common pre-processing step. Standardization is used in GNNs and linear regression, whereas no scaling is used for GBT.

4.3 | Performance Metrics

Two measures are used to evaluate the performance of the ML models. First, the coefficient of determination R^2 represents the proportion of the variation of the data explained by the model. A perfect model would have $R^2 = 1$, while a model that predicts the average of the test distribution achieves $R^2 = 0$.

Second, Spearman's rank correlation coefficient ρ is employed to assess whether the model correctly ranks the system components in terms of criticality. In many real-world applications, accurately identifying components most prone to fail is often more important than predicting the exact numerical values of stability measures. In this context, ML can serve as a tool for vulnerability detection.

For power grid applications, the aim is to predict which buses have the highest potential to destabilize the system. This allows grid operators that have to rely on limited computational resources to prioritize which configurations to analyse further. Combining ML predictions with more detailed simulations of the most vulnerable scenarios has the potential to improve grid operation.

5 | Results

5.1 | Numerical Results of Dynamical Simulations

First, the results of individual transients are introduced before considering multiple scenarios and studying the statistical properties of the datasets. Examples of individual transients of the dynamic simulations are shown in Figure 3. The binary classifiers for stability, given by the fault-ride-through curves introduced in Section 3.2, are evaluated for each simulation. The two cases visualize a stable and an unstable transient. The unstable transient exceeds the voltage ride-through limit.

We further analyse the dynamical behaviour by studying exemplary outcomes for three different bus types in Figure 4. Each fault results in a system-wide mismatch in active ΔP and reactive power ΔQ in the post-clearance states. The figure plots the post-clearance states in the ΔP - and ΔQ -plane. Solid and transparent markers represent post-clearance states that result in a successful and unsuccessful fault-ride-through.

Although the power differences are similar, the scenarios often result in different stability outcomes. The figures illustrate cases where larger magnitudes of power differences lead to stable outcomes, whereas more minor differences lead to instabilities. The behaviour is thus clearly non-linear. This shows that the outcome of individual fault scenarios is challenging to predict by solely looking at the magnitude of the fault. Dangerous situations might be missed when only analysing a small number of severe faults. This highlights the need for probabilistic stability analyses

TABLE 2 | Results of predicting p_{frit} using R^2 and ρ in % with different ML methods.

Model	Test R^2	IEEE R^2	Test ρ	IEEE ρ
linreg	62.11	72.02	74.56	81.86
GBT	62.99	72.17	74.81	76.13
DBGNN	96.68 ± 0.10	89.73 ± 3.77	98.03 ± 0.03	92.87 ± 1.96

to uncover critical components in the grid that may fail in a wide range of situations.

Finally, we discuss the statistical properties of the dataset. The histograms of p_{frit} are shown in Figure 5. We see that different time constants τ_p lead to different fault-ride-through behaviours. As expected, the buses with the highest time constant, NF3, lead to the highest mean fault-ride-through probability. All histograms show that the p_{frit} varies vastly for individual buses. Buses with the same machine parameters can either always successfully ride through a fault or might never, or anything in between. We clearly see an impact of the grid topologies on stability, which can not be explained at the individual component level. Hence, it is not sufficient to study only individual components; the topological embedding has to be considered as well.

The IEEE test case is slightly more stable ($\overline{p_{\text{frit}}} \approx 0.589$) in comparison to the synthetic power grids ($\overline{p_{\text{frit}}} \approx 0.522$). In general, such distribution shifts are challenging for the generalization capabilities of ML approaches because ML models are good at interpolating but struggle at extrapolating to unseen data. Hence, predicting the non-linear stability of the IEEE test case can be seen as a test for the generalization capabilities of the used ML models.

We see that our simulations feature both a non-linear dependence on the fault magnitudes and a clear impact of the topology on the stability outcomes. These results further motivate the probabilistic approach for determining stability. Because of the impact of the topology on the stability, we suspect that GNNs will have an advantage over the non-graph ML methods.

5.2 | ML Performance

The results in Table 2 show that all employed ML methods can predict p_{frit} and generalize to the IEEE test case. Importantly, no statistically solid conclusions can be drawn from a single IEEE test case as it only consists of 72 buses, respectively, data points. The IEEE test case should be considered as an illustration of strong generalization capabilities.

On the synthetic power grids, DBGNN clearly outperforms non-graph ML (regression and GBT). Figure 6 visualizes the performance of the DBGNN model. The majority of the predictions are around the diagonal line, indicating a high predictive performance. Considering the histograms of the labels (true p_{frit}), it can be seen that there are two peaks in the distributions representing less stable configurations (≈ 0.2) and more stable buses (≈ 0.9). Both peaks can be predicted correctly, as seen in the black regions, which indicate many predictions.

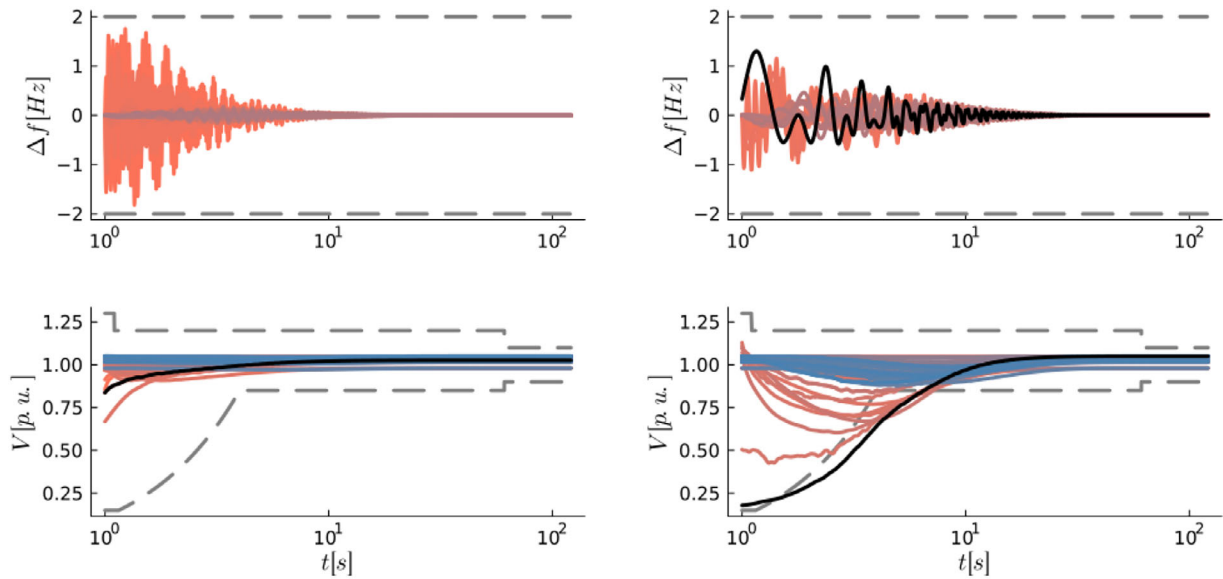


FIGURE 3 | Example transients of the dynamical simulations, visualized by the frequency deviation from the reference frequency of 50 Hz and the voltage magnitude V . The dashed line in gray shows the fault ride through curve. The black transients mark the bus where the fault occurred. The time is plotted on a logarithmic scale to highlight the first time steps. The plots visualize a stable configuration (left) and an unstable configuration (right), for which the voltage thresholds are exceeded.

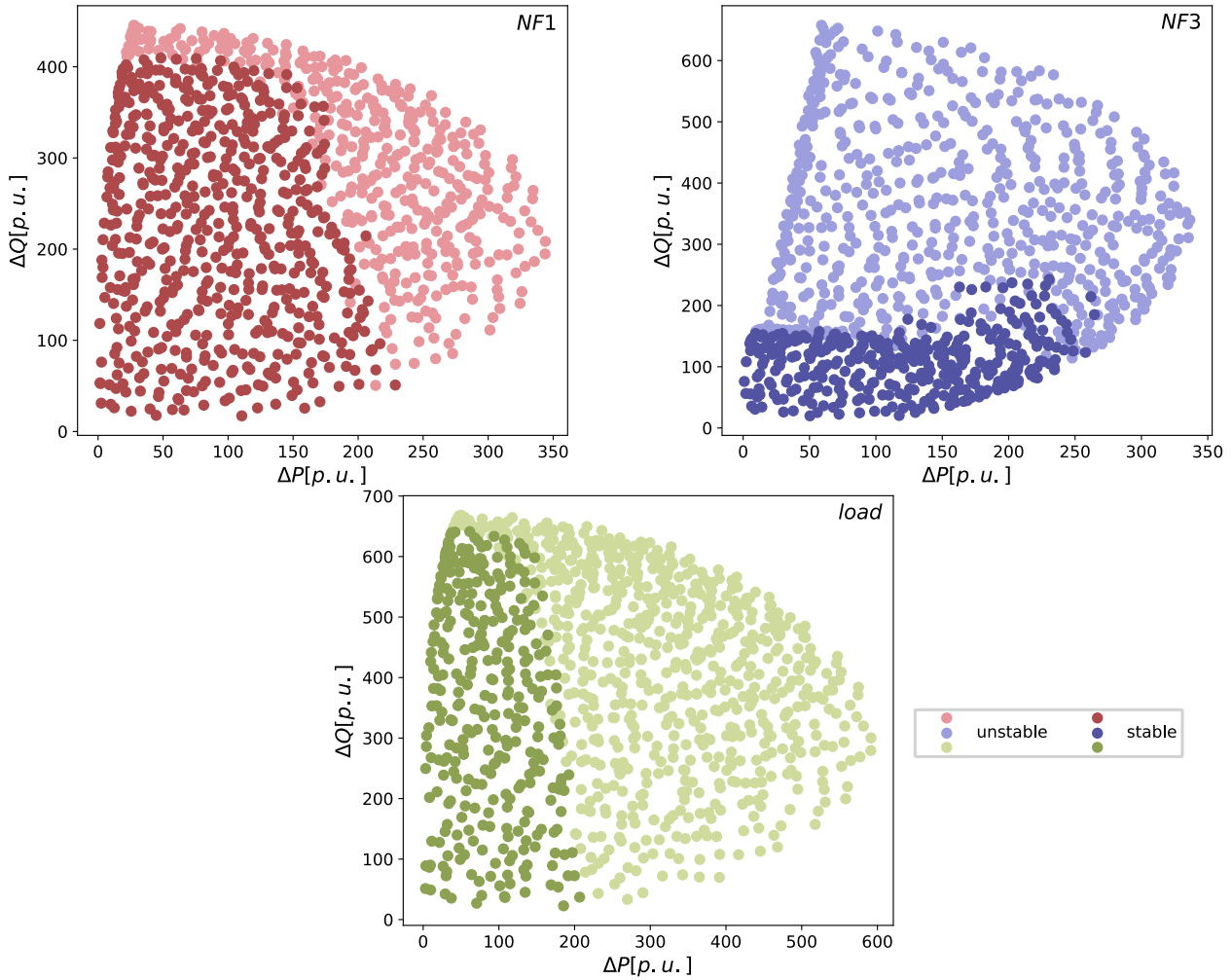


FIGURE 4 | The active and reactive power deviations ΔP and ΔQ resulting from the faults at three different buses of the IEEE test case, and the outcome of the corresponding simulations. Darker points indicate that the system survives and returns to stable operation, whereas light points indicate a failure. Colour distinguishes between the types of the shown buses, namely an NF1 bus (top left), an NF3 bus (top right) and a load bus (bottom).

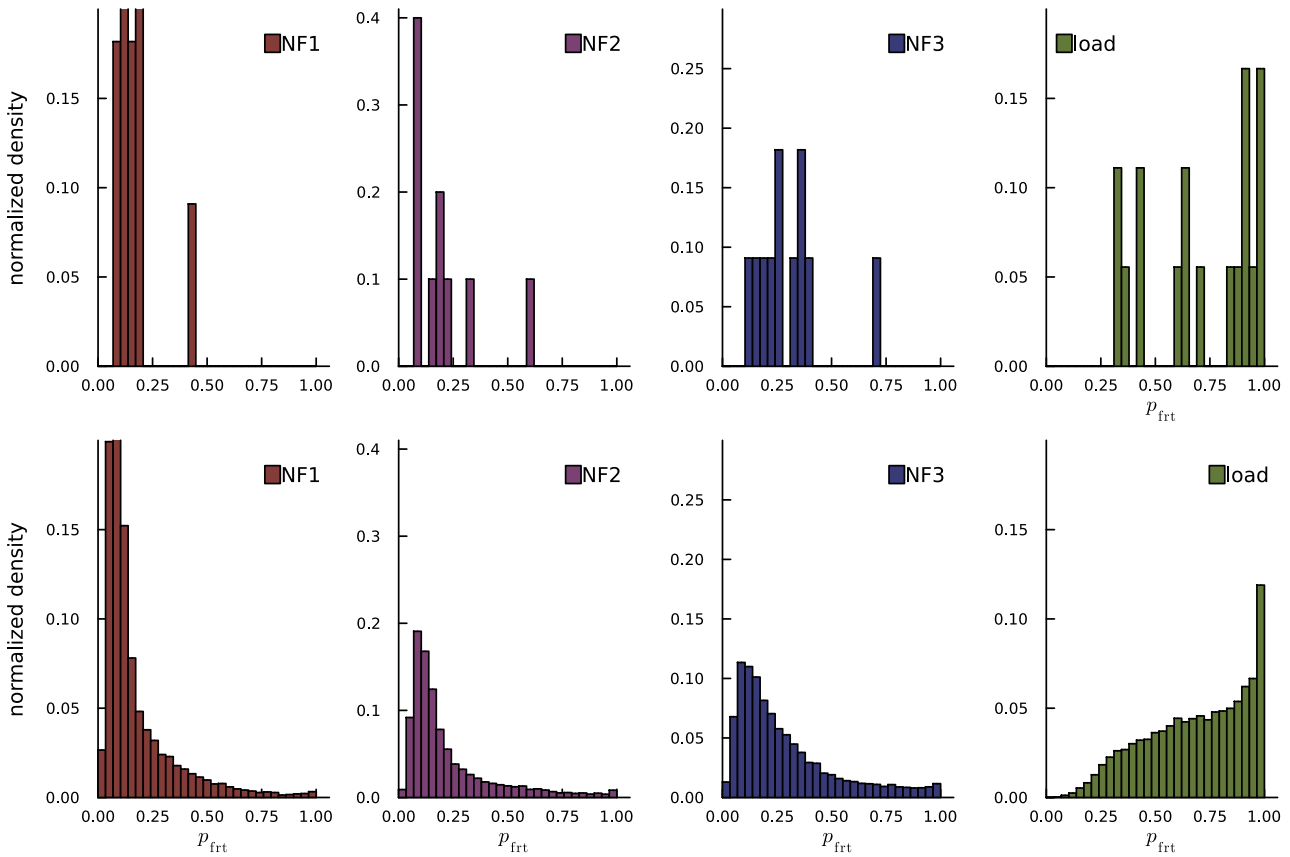


FIGURE 5 | The histograms of the p_{frt} for the IEEE test case are at the top, and for the 1000 synthetic grids are at the bottom. The columns depict the four different bus types. NF1–3 denotes the different normal-form parameterizations. For the loads, a different scaling of the vertical axis is used.

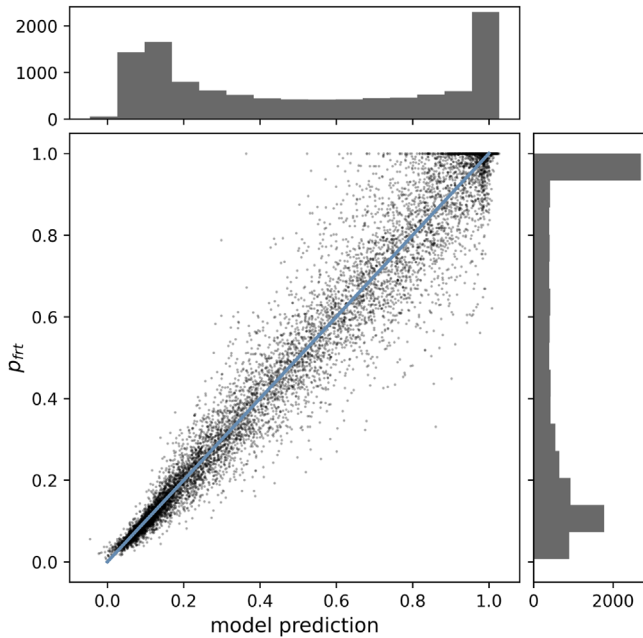


FIGURE 6 | Visualization of the performance of DBGNN. A perfect model would be on the diagonal blue line.

Importantly, DBGNN not only performs better on the synthetic datasets, but it also outperforms GBT and linreg on the IEEE test case. Hence, it generalizes well to an unknown configuration. The strong performance of DBGNN indicates DBGNN is capable

of recognizing topological patterns that impact p_{frt} as shown in Section 5.1. DBGNNs are particularly well-suited for modelling power grid dynamics due to their wave-like propagation mechanism, which naturally captures the physical propagation of disturbances through the network—unlike conventional diffusive GNN architectures. The parallel update of node and edge features enables DBGNNs to model the simultaneous evolution of bus states and power flows, which is fundamental to power system dynamics.

In general, the solid performance of all methods shows that ML can predict the non-linear stability of the IEEE case, even though its properties are quite different from the synthetic power grids. In contrast to GNNs, GBTs are known to perform well in sparse-data scenarios [51], suggesting they may be advantageous when sufficiently large datasets are unavailable.

6 | Conclusion

Analysing large sets of fault scenarios is required by ENTSO-E [8] to assess the stability of power grids, but the feasibility of such approaches has been limited by the high computational cost of dynamic simulations. This study demonstrates the potential of ML methods to efficiently predict the outcomes of probabilistic stability assessments and to prioritize scenarios for more detailed analysis, with a focus on the fault-ride-through probability (p_{frt}) in inverter-dominated power grids.

A novel, large dataset of inverter-based power grids was generated to train the ML models, capturing the relevance of topological structures and the non-linear nature of power system stability. All deployed ML methods were able to predict p_{frit} of the ensembles, with GNNs that incorporate topological features outperforming non-graph-based approaches. Importantly, the ML models demonstrated the ability to generalize to a differently structured IEEE test case was not included in the training set, highlighting the potential for applying models trained on synthetic data to real-sized power grids where probabilistic stability assessments are otherwise infeasible.

Conventional Monte Carlo simulations take approximately 50 CPU hours per grid with 70–80 nodes, while ML predictions complete in under a second per grid—enabling the exploration of virtually unlimited configurations at speeds unattainable with traditional methods. This dramatic speedup makes the automated analysis of numerous scenarios and identification of critical components prone to failure feasible for enhancing power grid operation. The demonstrated ability of ML models to accurately rank critical components and prioritize scenarios for detailed analysis provides an efficient framework for vulnerability detection. By leveraging ML to screen and prioritize the most vulnerable scenarios, grid operators can allocate expensive simulation resources where they matter most, enabling comprehensive contingency analysis that would be computationally infeasible with conventional approaches alone. This targeted approach allows operators to enhance system resilience by focusing preventive measures where they are most needed.

Author Contributions

Christian Nauck: conceptualization, data curation, investigation, methodology, visualization, writing – original draft, writing – review and editing. **Anna Büttner:** conceptualization, data curation, investigation, methodology, writing – original draft, writing – review and editing. **Sebastian Liemann:** research design, draft editing. **Frank Hellmann:** conceptualization, funding acquisition, resources, writing – review and editing. **Michael Lindner:** conceptualization, data curation, methodology, writing – review and editing.

Acknowledgements

All authors gratefully acknowledge Land Brandenburg for supporting this project by providing resources on the high-performance computer system at the Potsdam Institute for Climate Impact Research. The work was in parts supported by DFG Grant Number KU 837/39-2 (360460668), BMWK Grant 03EI1016A and BMBF Grant 03SF0766. Michael Lindner greatly acknowledges support from the Berlin International Graduate School in Model and Simulation (BIMoS) and his doctoral supervisor, Professor Eckehard Schöll. Christian Nauck would like to thank the German Federal Environmental Foundation (DBU) for funding his PhD scholarship and Professor Jörg Raisch for the supervision. Anna Büttner acknowledges support from the German Academic Scholarship Foundation and her doctoral supervisor, Professor Jürgen Kurths. AI tools, namely ChatGPT, Grammarly and llama3 are used to improve language. Open access funding enabled and organized by Projekt DEAL.

Funding

This work was supported by the German Research Foundation (DFG) under Grant No. KU 837/39-2 (360460668), the Federal Ministry for Economic Affairs and Climate Action (BMWK) under Grant No. 03EI1016A,

and the Federal Ministry of Education and Research (BMBF) under Grant No. 03SF0766. Michael Lindner received support from the Berlin International Graduate School in Model and Simulation (BIMoS). Christian Nauck was funded by a PhD scholarship from the German Federal Environmental Foundation (DBU). Anna Büttner received support from the German Academic Scholarship Foundation.

Conflicts of Interest

The authors declare no conflicts of interest.

Data Availability Statement

The code to generate the datasets and figures, as well as to train the ML models, is provided on GitHub and Zenodo.

References

1. F. Milano, F. Dörfler, G. Hug, D. J. Hill, and G. Verbič, “Foundations and Challenges of Low-Inertia Systems,” in *2018 Power Systems Computation Conference (PSCC)* (IEEE, 2018), 1–25.
2. T. Ackermann, G. Andersson, and L. Söder, “Distributed Generation: A Definition1,” *Electric Power Systems Research* 57, no. 3 (2001): 195–204.
3. K. Engeland, M. Borga, J.-D. Creutin, B. François, M.-H. Ramos, and J.-P. Vidal, “Space-Time Variability of Climate Variables and Intermittent Renewable Electricity Production – A Review,” *Renewable and Sustainable Energy Reviews* 79 (2017): 600–617.
4. A. M. Saleh, I. Vokony, M. Waseem, M. A. Khan, and A. Al-Areqi, “Power System Stability With High Integration of RESs and EVs: Benefits, Challenges, Tools, and Solutions,” *Energy Reports* 13 (2025): 2637–2663.
5. “High Penetration of Power Electronic Interfaced Power Sources and the Potential Contribution of Grid Forming Converters,” ENTSO-E, published January 30, 2020, https://eepublicdownloads.entsoe.eu/clean-documents/Publications/SOC/High_Penetration_of_Power_Electronic_Interfaced_Power_Sources_and_the_Potential_Contribution_of_Grid_Forming_Converters.pdf.
6. D. Witthaut, F. Hellmann, J. Kurths, S. Kettmann, H. Meyer-Ortmanns, and M. Timme, “Collective Nonlinear Dynamics and Self-Organization in Decentralized Power Grids,” *Reviews of Modern Physics* 94, no. 1 (2022): 015005, <https://doi.org/10.1103/RevModPhys.94.015005>.
7. “SPD DSA Task Force Dynamic Security Assessment (DSA),” ENTSO-E, published April 17, 2017, https://eepublicdownloads.entsoe.eu/clean-documents/SOC%20documents/Regional_Groups_Continental_Europe/2017/DSA_REPORT_Public.pdf.
8. “All Continental Europe and Nordic TSOs’ Proposal for Assumptions and a Cost Benefit Analysis Methodology in Accordance With Article 156(11) of the Commission Regulation (EU) 2017/1485 of 2 August 2017 Establishing a Guideline on Electricity Transmission System Operation,” ENTSO-E, published January 10, 2018, https://eepublicdownloads.entsoe.eu/clean-documents/nc-tasks/EBGL/SOGL_156.11_CBA%20for%20FCR%20by%20LER_all%20CE%20and%20Nordic%20TSOs_legal%20document_after%20RfA_CLEAN.pdf.
9. J. Xie, I. Alvarez-Fernandez, and W. Sun, “A Review of Machine Learning Applications in Power System Resilience,” in *2020 IEEE Power & Energy Society General Meeting (PESGM)* (IEEE, 2020), 1–5, <https://doi.org/10.1109/pesgm41954.2020.9282137>.
10. W. Liao, B. Bak-Jensen, J. R. Pillai, Y. Wang, and Y. Wang, “A Review of Graph Neural Networks and Their Applications in Power Systems,” *Journal of Modern Power Systems and Clean Energy* 10, no. 2 (2022): 345–360, <https://doi.org/10.35833/MPCE.2021.000058>.
11. C. Cambier van Nooten, T. Poll, S. Füllhase, J. Heres, T. Heskes, and Y. Shapovalova, “Graph Neural Networks for Assessing the Reliability of the Medium-Voltage Grid,” *Applied Energy* 384 (2025): 125401, <https://doi.org/10.1016/j.apenergy.2025.125401>.

12. B. Borkowska, "Probabilistic Load Flow," *IEEE Transactions on Power Apparatus and Systems* PAS-93, no. 3 (1974): 752–759, <https://doi.org/10.1109/TPAS.1974.293973>.
13. H.-Y. Su and H.-H. Hong, "An Intelligent Data-Driven Learning Approach to Enhance Online Probabilistic Voltage Stability Margin Prediction," *IEEE Transactions on Power Systems* 36, no. 4 (2021): 3790–3793, <https://doi.org/10.1109/TPWRS.2021.3067150>.
14. J. Huang, L. Guan, Y. Su, H. Yao, M. Guo, and Z. Zhong, "Recurrent Graph Convolutional Network-Based Multi-Task Transient Stability Assessment Framework in Power System," *IEEE Access* 8 (2020): 93283–93296, <https://doi.org/10.1109/ACCESS.2020.2991263>.
15. J. Qiao, X. Wang, J. Ni, M. Shi, H. Ren, and E. Chen, "Graph Neural Network Based Transient Stability Assessment Considering Topology Changes," in *2021 International Conference on Power System Technology (POWERCON)* (IEEE, 2021), 1999–2003, <https://doi.org/10.1109/POWERCON53785.2021.9697706>.
16. E. S. Kiel, S. H. Jakobsen, E. Haugen, S. D. Lundemo, S. Riemersørensen, and F. Remonato, "A Tree Based Classifier for Transient Stability Prediction Following Island Splitting," in *2022 17th International Conference on Probabilistic Methods Applied to Power Systems (PMAPS)* (IEEE, 2022), 1–6, <https://doi.org/10.1109/PMAPS53380.2022.9810650>.
17. E. A. S. Ducoin, Y. Gu, B. Chaudhuri, and T. C. Green, "Analytical Design of Contributions of Grid-Forming and Grid-Following Inverters to Frequency Stability," *IEEE Transactions on Power Systems* 39, no. 5 (2024): 6345–6358, <https://doi.org/10.1109/TPWRS.2024.3351530>.
18. K. Singh, A. Tank, R. Mohanty, A. Tripathi, and A. Verma, "Frequency Response Assessment of Inverter Dominated Power System Under Grid Abnormalities," in *2024 IEEE International Conference on Power Electronics, Drives and Energy Systems (PEDES)* (IEEE, 2024), 1–6, <https://doi.org/10.1109/PEDES61459.2024.10961347>.
19. A. Panwar, Z. H. Rather, S. Doolla, A. Liebman, and R. Dargaville, "A Machine Learning Based Approach for Frequency Response Prediction in Low Inertia Power System," in *2022 IEEE PES Innovative Smart Grid Technologies - Asia (ISGT Asia)* (IEEE, 2022), 175–179, <https://doi.org/10.1109/ISGTAsia54193.2022.10003489>.
20. C. Nauck, M. Lindner, K. Schürholt, and F. Hellmann, "Towards Dynamic Stability Analysis of Sustainable Power Grids Using Graph Neural Networks," preprint, arXiv, December 22, 2022, <https://doi.org/10.48550/arXiv.2212.11130>.
21. M. Titz, F. Kaiser, J. Kruse, and D. Witthaut, "Predicting Dynamic Stability From Static Features in Power Grid Models Using Machine Learning," *Chaos: An Interdisciplinary Journal of Nonlinear Science* 34, no. 1 (2024): 013139, <https://doi.org/10.1063/5.0175372>.
22. F. Hellmann, P. Schultz, C. Grabow, J. Heitzig, and J. Kurths, "Survivability of Deterministic Dynamical Systems," *Scientific Reports* 6, no. 1 (2016): 29654, <https://doi.org/10.1038/srep29654>.
23. J. Nitzbon, P. Schultz, J. Heitzig, J. Kurths, and F. Hellmann, "Deciphering the Imprint of Topology on Nonlinear Dynamical Network Stability," *New Journal of Physics* 19, no. 3 (2017): 033029, <https://doi.org/10.1088/1367-2630/aa6321>.
24. L. Strenge, H. Kirchhoff, G. L. Ndow, and F. Hellmann, "Stability of Meshed DC Microgrids Using Probabilistic Analysis," in *2017 IEEE Second International Conference on DC Microgrids (ICDCM)* (IEEE, 2017), 175–180, <https://doi.org/10.1109/ICDCM.2017.8001040>.
25. S. Liemann, L. Strenge, P. Schultz, et al., "Probabilistic Stability Assessment for Active Distribution Grids," in *2021 IEEE Madrid PowerTech* (IEEE, 2021), 1–6, <https://doi.org/10.1109/PowerTech46648.2021.9494855>.
26. Q.-H. Ngo, B. L. H. Nguyen, T. V. Vu, J. Zhang, and T. Ngo, "Physics-Informed Graphical Neural Network for Power System State Estimation," *Applied Energy* 358 (2024): 122602, <https://doi.org/10.1016/j.apenergy.2023.122602>.
27. D. Harrison-Atlas, A. Glaws, R. N. King, and E. Lantz, "Artificial Intelligence-Aided Wind Plant Optimization for Nationwide Evaluation of Land Use and Economic Benefits of Wake Steering," *Nature Energy* 9, no. 6 (2024): 735–749, <https://doi.org/10.1038/s41560-024-01516-8>.
28. A. Varbella, K. Amara, B. Gjorgiev, and G. Sansavini, "PowerGraph: A Power Grid Benchmark Dataset for Graph Neural Networks," preprint, arXiv, February 5, 2024, <https://doi.org/10.48550/arXiv.2402.02827>.
29. Y. Zhang, P. M. Karve, and S. Mahadevan, "Graph Neural Networks for Power Grid Operational Risk Assessment Under Evolving Unit Commitment," *Applied Energy* 380 (2025): 124793, <https://doi.org/10.1016/j.apenergy.2024.124793>.
30. C. Nauck, R. Gorantla, M. Lindner, K. Schurholt, A. S. J. S. Mey, and F. Hellmann, "Dirac–Bianconi Graph Neural Networks – Enabling Non-Diffusive Long-Range Graph Predictions," in *Proceedings of the Geometry-grounded Representation Learning and Generative Modeling Workshop (GRAm)* (PMLR, 2024), 146–157, <https://proceedings.mlr.press/v251/nauck24a.html>.
31. R. Billinton and W. Li, *Reliability Assessment of Electric Power Systems Using Monte Carlo Methods* (Springer, 1994), <https://doi.org/10.1007/978-1-4899-1346-3>.
32. T. Qoria, Q. Cossart, C. Li, X. Guillaud, F. Gruson, and X. Kestelyn, *WP3 - Control and Operation of a Grid with 100 Converter-Based Devices* (H2020 MIGRATE Project, 2018), https://www.h2020-migrate.eu/_Resources/Persistent/1bb0f89024e41a85bf94flec7ee6f8d7c34bc29a/D3.6%20-%20Requirement%20guidelines%20for%20operating%20a%20grid%20with%20100%20power%20electronic%20devices.pdf.
33. VDE, *FNN Guideline: Grid Forming Behaviour of HVDC Systems and DC-Connected PPMs* (VDE Publishing House, 2020), <https://shop.vde.com/en/fnn-guideline-hvdc-systems-2>.
34. VDE, *Technical Connection Rules for HVDC Systems and via HVDC Systems Connected Generation Plants* (VDE Verlag, 2019), <https://www.vde-verlag.de/normen/0100511/vde-ar-n-4131-anwendungsregel-2019-03.html>.
35. A. Kumbhar, P. G. Dhawale, S. Kumbhar, U. Patil, and P. Magdum, "A Comprehensive Review: Machine Learning and Its Application in Integrated Power System," *Energy Reports* 7 (2021): 5467–5474, <https://doi.org/10.1016/j.egy.2021.08.133>.
36. T. N. Kipf and M. Welling, "Semi-Supervised Classification with Graph Convolutional Networks," preprint, arXiv, February 20, 2017, <http://arxiv.org/abs/1609.02907>.
37. M. Ringsquandl, H. Sellami, M. Hildebrandt, et al., "Power to the Relational Inductive Bias: Graph Neural Networks in Electrical Power Grids," in *Proceedings of the 30th ACM International Conference on Information & Knowledge Management*, (Association for Computing Machinery, 2021), 1538–1547, <https://doi.org/10.1145/3459637.3482464>.
38. A. Büttner, A. Plietzsch, M. Anvari, and F. Hellmann, "A Framework for Synthetic Power System Dynamics," *Chaos: An Interdisciplinary Journal of Nonlinear Science* 33, no. 8 (2023): 083120, <https://doi.org/10.1063/5.0155971>.
39. J. Schiffer, R. Ortega, A. Astolfi, J. Raisch, and T. Sezi, "Conditions for Stability of Droop-Controlled Inverter-Based Microgrids," *Automatica* 50, no. 10 (2014): 2457–2469, <https://doi.org/10.1016/j.automatica.2014.08.009>.
40. R. Kogler, A. Plietzsch, P. Schultz, and F. Hellmann, "Normal Form for Grid-Forming Power Grid Actors," *PRX Energy* 1, no. 1 (2022): 013008, <https://doi.org/10.1103/PRXEnergy.1.013008>.
41. A. Büttner, H. Würfel, S. Liemann, J. Schiffer, and F. Hellmann, "Complex-Phase, Data-Driven Identification of Grid-Forming Inverter Dynamics," *IEEE Transactions on Smart Grid* 16, no. 6 (2024): 4854–4864, <https://doi.org/10.48550/arXiv.2409.17132>.
42. A. Büttner, J. Kurths, and F. Hellmann, "Ambient Forcing: Sampling Local Perturbations in Constrained Phase Spaces," *New Journal of Physics* 24, no. 5 (2022): 053019, <https://doi.org/10.1088/1367-2630/ac6822>.
43. P. Schultz, J. Heitzig, and J. Kurths, "A Random Growth Model for Power Grids and Other Spatially Embedded Infrastructure Networks,"

European Physical Journal Special Topics 223, no. 12 (2014): 2593–2610, <https://doi.org/10.1140/epjst/e2014-02279-6>.

44. dena, *dena-Verteilnetzstudie: Ausbau- und Innovationsbedarf der Stromverteilnetze in Deutschland bis 2030* (Deutsche Energie-Agentur GmbH, 2012), <https://www.dena.de/newsroom/publikationsdetailansicht/pub/dena-verteilstudie-ausbau-und-innovationsbedarf-der-stromverteilnetze-in-deutschland-bis-2030/>.

45. J. Egerer, *DIW Berlin: Open Source Electricity Model for Germany (ELMOD-DE)* (DIW Berlin, 2016), https://www.diw.de/de/diw_01.c.528929.de/publikationen/data_documentation/2016_0083/open_source_electricity_model_for_germany_elmod-de.html.

46. H. Taher, S. Olmi, and E. Schöll, “Enhancing Power Grid Synchronization and Stability Through Time-Delayed Feedback Control,” *Physical Review E* 100, no. 6 (2019): 062306, <https://doi.org/10.1103/PhysRevE.100.062306>.

47. W. Zhang, F. Li, and L. M. Tolbert, “Review of Reactive Power Planning: Objectives, Constraints, and Algorithms,” *IEEE Transactions on Power Systems* 22, no. 4 (2007): 2177–2186, <https://doi.org/10.1109/TPWRS.2007.907452>.

48. VDE, *Technical Connection Rules for Medium-Voltage (VDE-AR-n 4110)* (VDE Publishing House, 2018), <https://www.vde.com/en/fnn/topics/technical-connection-rules/tcr-for-medium-voltage>.

49. I. M. Sobol’, “On the Distribution of Points in a Cube and the Approximate Evaluation of Integrals,” *USSR Computational Mathematics and Mathematical Physics* 7, no. 4 (1967): 86–112, [https://doi.org/10.1016/0041-5553\(67\)90144-9](https://doi.org/10.1016/0041-5553(67)90144-9).

50. C. Grigg, P. Wong, P. Albrecht, et al., “The IEEE Reliability Test System-1996. A Report Prepared by the Reliability Test System Task Force of the Application of Probability Methods Subcommittee,” *IEEE Transactions on Power Systems* 14, no. 3 (1999): 1010–1020, <https://doi.org/10.1109/59.780914>.

51. C. Nauck, M. Lindner, N. Molkenhain, et al., “Predicting Instability in Complex Oscillator Networks: Limitations and Potentials of Network Measures and Machine Learning,” preprint, arXiv, February 27, 2024, <http://arxiv.org/abs/2402.17500>.

52. “PIK-ICoNe/FaultRideThroughProbabilityML_paper-companion,” GitHub repository, published December 2024, https://github.com/PIK-ICoNe/FaultRideThroughProbabilityML_paper-companion.

53. C. Nauck, A. Büttner, S. Liemann, M. Lindner, and F. Hellmann, “Predicting Fault-Ride-Through Probability of Inverter-Dominated Power Grids Using Machine Learning,” Zenodo, published May 25, 2024, <https://doi.org/10.5281/zenodo.11193717>.

54. A. Plietzsch, R. Kogler, S. Auer, et al., “PowerDynamics.jl—An Experimentally Validated Open-Source Package for the Dynamical Analysis of Power Grids,” *SoftwareX* 17 (2022): 100861, <https://doi.org/10.1016/j.softx.2021.100861>.

55. M. Lindner, L. Lincoln, F. Drauschke, et al., “NetworkDynamics.jl—Composing and Simulating Complex Networks in Julia,” *Chaos: An Interdisciplinary Journal of Nonlinear Science* 31, no. 6 (2021): 063133, <https://doi.org/10.1063/5.0051387>.

56. C. Rackauckas and Q. Nie, “DifferentialEquations.jl – A Performant and Feature-Rich Ecosystem for Solving Differential Equations in Julia,” *Journal of Open Research Software* 5, no. 1 (2017): 15, <https://doi.org/10.5334/jors.151>.

57. A. Paszke, S. Gross, F. Massa, et al., “PyTorch: An Imperative Style, High-Performance Deep Learning Library,” in *Advances in Neural Information Processing Systems*, ed. H. Wallach, H. Larochelle, A. Beygelzimer, F. Alché-Buc, E. Fox, and R. Garnett (Curran Associates, Inc., 2019), 8024–8035, <http://papers.nips.cc/paper/9015-pytorch-an-imperative-style-high-performance-deep-learning-library.pdf>.

58. M. Fey and J. E. Lenssen, “Fast Graph Representation Learning with PyTorch Geometric,” preprint, arXiv, March 6, 2019, <https://doi.org/10.48550/ARXIV.1903.02428>.

59. P. Moritz, R. Nishihara, S. Wang, et al., “Ray: A Distributed Framework for Emerging AI Applications,” preprint, arXiv, September 24, 2018, <http://arxiv.org/abs/1712.05889>.

60. R. Liaw, E. Liang, R. Nishihara, P. Moritz, J. E. Gonzalez, and I. Stoica, “Tune: A Research Platform for Distributed Model Selection and Training,” preprint, arXiv, July 13, 2018, <https://doi.org/10.48550/arXiv.1807.05118>.

61. G. E. Hinton, N. Srivastava, A. Krizhevsky, I. Sutskever, and R. R. Salakhutdinov, “Improving neural networks by preventing co-adaptation of feature detectors,” preprint, arXiv, July 12, 2012, <http://arxiv.org/abs/1207.0580>.

Appendix A

A.1 | Data and Source Code Availability

To evaluate, validate and extend our work, we provide the code to generate the datasets and figures, as well as to train the ML models, on GitHub [52] and Zenodo [53].

A.2 | Details on Generating the Datasets

To generate the datasets, Julia 1.9.1 and the packages PowerDynamics.jl [54] and NetworkDynamics.jl [55], that heavily rely on DifferentialEquations.jl [56], were used for solving differential equations.

A.3 | Training Details

This section includes more information to reproduce the obtained results. For the training, Pytorch [57] is used. For the graph handling and graph convolutional layers, the library PyTorch Geometric [58] is used.

A.3.1 | Hyperparameter Study

ML models and their training are characterized by so-called hyperparameters. Hyperparameters are not learnable during the training but are distinctive for the behaviour, for example, by specifying the size of the models. Hyperparameter studies are conducted to optimize the performance by varying the number of hidden dimensions, scaling strategies, learning rates, dropout and model-specific parameters. For the hyperparameter study, ray [59] and tune [60] are used.

A.3.2 | Final Properties of the Model

The DBGNN consists of two layers, each with 30 steps. The hidden dimension for both nodes and edges is set to 120, with dropout rates of 0.014877 for nodes and 0.002454 for edges. Skip connections are applied throughout the network. The model comprises 147,961 learnable parameters. For training, the ADAM optimizer with a one-cycle learning rate policy and gradient clipping is utilized.

A.4 | Details on Dirac–Bianconi Graph Neural Networks

This section provides a brief overview of Dirac–Bianconi Graph Neural Networks (DBGNNs), introduced in [30]. DBGNNs employ a distinctive architecture where node and edge features are updated in parallel rather than sequentially. Unlike conventional GNNs that rely on diffusive feature propagation, DBGNNs support wave-like propagation dynamics. This wave-based mechanism naturally circumvents the oversmoothing and oversquashing problems that plague many GNNs, enabling effective long-range feature propagation.

A.4.1 | Mathematical Formulation

Let d_n and d_e denote the dimensions of node and edge feature spaces, respectively, so that $F_n = \mathbb{R}^{d_n}$ and $F_e = \mathbb{R}^{d_e}$. The DBGNN updates are governed by the generalized linear Dirac–Bianconi equations:

$$\mathbf{x}_i(t+1) = \mathbf{x}_i(t) + \mathbf{W}^{ne} \sum_{j \in \mathcal{N}_i} \mathbf{e}_{ij}(t) + \mathbf{W}_\beta^n \mathbf{x}_i(t), \quad (\text{A.1})$$

$$\mathbf{e}_{ij}(t+1) = \mathbf{e}_{ij}(t) + \mathbf{W}^{en}(\mathbf{x}_i(t) - \mathbf{x}_j(t)) - \mathbf{W}_\beta^e \mathbf{e}_{ij}(t),$$

where the coupling matrices $\mathbf{W}^{ne} \in \mathbb{R}^{d_n \times d_e}$ and $\mathbf{W}^{en} \in \mathbb{R}^{d_e \times d_n}$ mediate node-edge interactions, and the mass matrices $\mathbf{W}_\beta^n \in \mathbb{R}^{d_n \times d_n}$ and $\mathbf{W}_\beta^e \in \mathbb{R}^{d_e \times d_e}$ regulate self-feedback.

The node update depends on three components: the current node features $\mathbf{x}_i(t)$, the aggregated edge features $\sum_{j \in \mathcal{N}_i} \mathbf{e}_{ij}(t)$ mapped to node space via \mathbf{W}^{ne} , and a self-interaction term governed by \mathbf{W}_β^n . Similarly, the edge update incorporates the current edge features, self-interaction via \mathbf{W}_β^e , and the node feature difference $\mathbf{x}_i(t) - \mathbf{x}_j(t)$ mapped to edge space by \mathbf{W}^{en} .

The four coupling and mass matrices— \mathbf{W}^{ne} , \mathbf{W}^{en} , \mathbf{W}_β^n , and \mathbf{W}_β^e —constitute the learnable parameters of this layer.

A.5 | Regularization Methods for ML

One of the common problems of ML is the tendency of overfitting. By overfitting, we mean a process during training when the performances on the training set increase, whereas the validation and test performances do not increase anymore. To avoid models from simply memorizing the training data, dropout [61] is a widely used regularization method. The concept of dropout is applied during training when a pre-defined ratio of neurons is randomly deactivated.

A.6 | Declaration of Generative AI and AI-Assisted Technologies in the Writing Process

During the preparation of this work, the authors used ChatGPT, Grammarly and llama3 in order to improve the language. After using these services, the authors reviewed and edited the content as needed and take full responsibility for the content of the publication.